# Structure-Based Exploration of Cyclic Dipeptide Chitinase Inhibitors

Douglas R. Houston,[†] Bjørnar Synstad,[‡] Vincent G. H. Eijsink,[‡] Michael J. R. Stark,[§] Ian M. Eggleston,[†] and Daan M. F. van Aalten*,[†]

*Division of Biological Chemistry and Molecular Microbiology and Division of Gene Regulation and Expression, School of Life Sciences, University of Dundee, Dundee DD1 5EH, Scotland, U.K., and Department of Chemistry and Biotechnology, Agricultural University of Norway, N-1432 Ås, Norway*

*Received January 20, 2004*

Family 18 chitinases play an essential role in a range of pathogens and pests. Several inhibitors are known, including the potent inhibitors argadin and allosamidin, and the structures of these in complex with chitinases have been elucidated. Recent structural analysis has revealed that CI-4 [cyclo-(L-Arg-D-Pro)] inhibits family 18 chitinases by mimicking the structure of the proposed reaction intermediate. Here we report the high-resolution structures of four new CI-4 derivatives, cyclo-(L-Arg-L-Pro), cyclo-(Gly-L-Pro), cyclo-(L-His-L-Pro), and cyclo-(L-Tyr-L-Pro), in complex with a family 18 chitinase. In addition, details of enzyme inhibition and *in vivo* activity against *Saccharomyces cerevisiae* are presented. The structures reveal that the common cyclo-(Gly-Pro) substructure is sufficient for binding, allowing modification of the side chain of the nonproline residue. This suggests that design of cyclic dipeptides with a view to increasing inhibition of family 18 chitinases should be possible through relatively accessible chemistry. The derivatives presented here in complex with chitinase B from *Serratia marcescens* provide further insight into the mechanism of inhibition of chitinases by cyclic dipeptides as well as providing a new scaffold for chitinase inhibitor design.

## Introduction

Chitin, the linear polymer of *N*-acetylglucosamine, is an essential structural component of fungal, nematodal, and insect pathogens. Chitinases, which hydrolyze this polymer, play a key role in the life cycle of these pathogens and associated pathogenesis. For example, the malaria parasite *Plasmodium falciparum* secretes chitinase in order to penetrate the chitinous peritrophic matrix and infect the mosquito vector.[1,2] The fungal human pathogen *Candida albicans* utilizes chitinases during cell division to separate daughter cells.[3] Insect ecdysis also relies on chitinases.[4] The eggs of the nematode gastrointestinal parasite of mice, *Heligmosomoides polygyrus*, express increasing levels of chitinase with age up to hatching,[5] and *Entamoeba invadens*, a model for pathogenic amoebic encystation, produces chitinase during encystation.[6] Allosamidin, the first chitinase inhibitor to be discovered, is a potent broad-spectrum chitinase inhibitor in the nano- to micromolar range[7] that blocks or slows all of the above-mentioned essential physiological processes.[5,8−10] Unfortunately, allosamidin is no longer commercially available and its synthesis is complicated.[11,12] Further screening for natural product inhibitors of chitinases has also identified the cyclic pentapeptides argadin[13] and argifin,[14] allosamidin derivatives,[11,15,16] styloguanidines,[17] and the cyclic dipeptide CI-4 (cyclo-(L-Arg-D-Pro), Figure 1), for which total synthesis has been reported.[18,19] CI-4 inhibits *Saccharomyces cerevisiae* cell separation and prevents *C. albicans* from entering its infectious filamentous form.[19]

The family 18 chitinase retaining reaction mechanism proceeds via an unusual oxazolinium intermediate.[20−23] This intermediate is formed when the *N*-acetyl group of the *N*-acetylglucosamine bound in the −1 subsite, carries out a nucleophilic attack on the anomeric carbon. The resulting structure, a five-membered oxazoline ring fused to a pyranose ring (Figure 1), is similar to allosamidin, one of the most potent chitinase inhibitors[7] (Figure 1). The structure of the natural product chitinase inhibitor CI-4 (cyclo-(L-Arg-D-Pro), Figure 1) bound to chitinase B from *Serratia marcescens* (ChiB) was described recently, showing that CI-4 binds to ChiB by mimicking the structures and binding modes of allosamidin and the catalytic intermediate[24] (Figures 1 and 2). Although CI-4 inhibition was poor ($IC_{50}$ = 1.2 mM), it is a potentially interesting lead because of its relatively accessible chemical makeup, thus making it a useful scaffold for derivatization.

Structure-based optimization of CI-4 requires an understanding of the characteristics of CI-4 that are essential for binding. From the complex of CI-4 with ChiB, it appears that CI-4 possesses two major features: a cyclo-(Gly-Pro) backbone and an arginine side chain (Figures 1 and 2). A comparison of CI-4's cyclic dipeptide backbone with the catalytic intermediate structure suggests that it is this backbone alone that most closely resembles the catalytic intermediate and the allosamizolin moiety of allosamidin (Figure 1). The arginine side chain in the CI-4 structure is less ordered and does not hydrogen bond the protein directly (Figures 1 and 2). This suggests that the arginine may not be essential for binding and could be a suitable site for derivatization and/or change of stereochemistry. The

* To whom correspondence should be addressed. Tel.: ++ 44 1382 344979. Fax: ++ 44 1382 345764. E-mail: dava@davapc1.bioch.dundee.ac.uk.

[†] Division of Biological Chemistry and Molecular Microbiology, University of Dundee.

[‡] Agricultural University of Norway.

[§] Division of Gene Regulation and Expression, University of Dundee.

10.1021/jm049940a CCC: $27.50 
Published on Web 10/09/2004

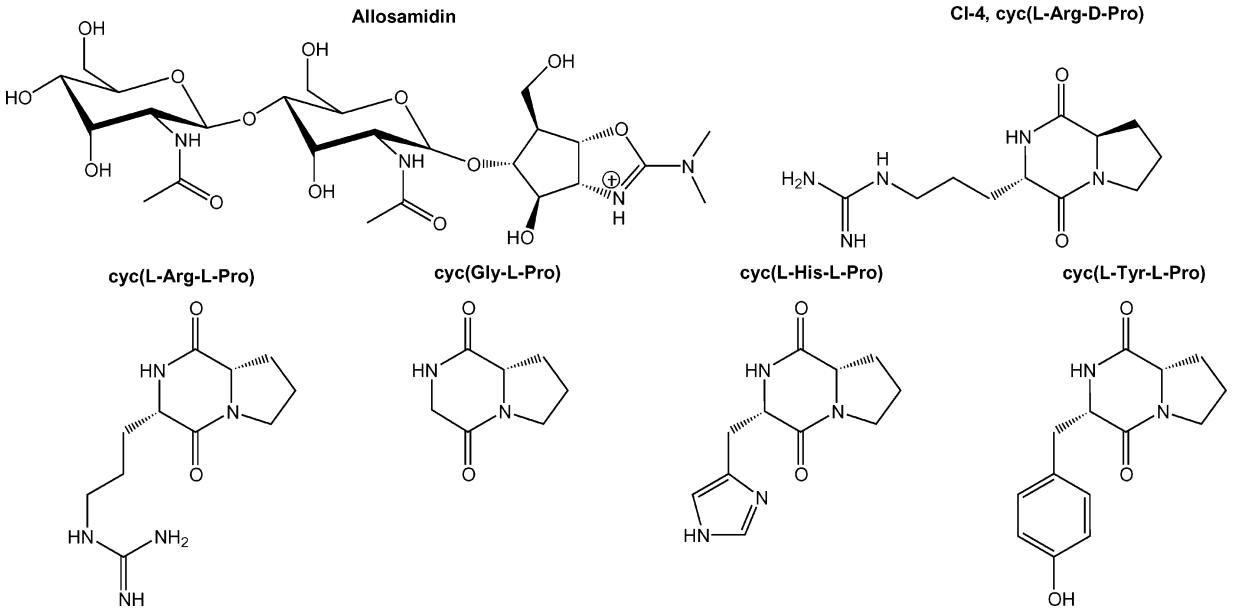


**Figure 1.** Comparison of the allosamidin and cyclic dipeptide chemical structures.

report of the discovery of CI-4 as a chitinase inhibitor also describes the effect of cyclo-(L-Arg-L-Pro) (a stereoisomer of CI-4, Figure 1) on chitinase activity, observing that it was at least as potent an inhibitor as CI-4.[19] Here, we describe the structure of this molecule in complex with ChiB. To confirm the role of the cyclic backbone in binding, the structure of ChiB in complex with cyclo-(Gly-L-Pro) was also determined. In addition, the effects of two alternative side chains were investigated by elucidating the structures of cyclo-(L-His-L-Pro) and cyclo-(L-Tyr-L-Pro) bound to ChiB (Figure 1). Inhibition data for these four cyclic dipeptides are reported, and we propose an explanation for the differences in potency between these dipeptides and allosamidin. The most potent dipeptide reported here is cyclo-(L-His-L-Pro), where the ordered histidine side chain makes several contacts with active site residues. This compound is also shown to affect *S. cerevisiae* cell separation. Together, the structural and biochemical data show that the cyclo-(Gly-L-Pro) scaffold is a useful template for further optimization and that inhibitory potential can be tuned by varying the second amino acid side chain.

## Results and Discussion

Four cyclic dipeptides related to CI-4 (Figure 1) were cocrystallized with chitinase B from *S. marcescens* (ChiB). Synchrotron diffraction data were collected and the complexes were refined to high resolution (between 1.85 and 2.1 Å), with good *R*-factors and geometry (see Table 1 in the Supporting Information). All the dipeptides were well-defined by unbiased $|F_o| - |F_c|$, $\phi_{calc}$ electron density maps (Figures 2 and 3) and bound in the same site as previously observed in the ChiB−CI-4 complex.[24] The maps allowed unambiguous verification of the stereochemistry of the compounds (Figures 2 and 3). To evaluate the potency of these dipeptides as chitinase inhibitors, their $IC_{50}$'s were determined using a standard fluorescence-based assay (Figure 4). Below, the structural analysis and comparisons are described for each of the dipeptides.

**Cyclo-(L-Arg-L-Pro).** The inhibition of *Bacillus* sp. chitinase by cyclo-(L-Arg-L-Pro) was reported as being approximately the same as CI-4 (in which the proline is the D stereoisomer, Figure 1), implying that it is possible to change the stereochemistry of the proline Cα-carbon and retain activity.[19] Cyclo-(L-Arg-L-Pro) was synthesized and purified and the structure of its complex with ChiB refined to 2.1 Å resolution (Figure 2). The structure shows that the change in chirality of the proline changes the binding orientation of the cyclo-(Gly-Pro) substructure. Compared to CI-4, cyclo-(L-Arg-L-Pro) is rotated 180° so that the arginine side chain is pointing toward the + subsites, rather than the − subsites as in the CI-4-ChiB complex (Figure 2). However, the number and nature of the interactions that CI-4 and cyclo-(L-Arg-L-Pro) make from their cyclic dipeptide backbone to the protein are essentially the same (Figure 2). The carbonyl group of the CI-4 arginine makes a hydrogen bond with the backbone nitrogen of Trp97, whereas in cyclo-(L-Arg-L-Pro) this is replaced with a similar hydrogen bond made from the proline carbonyl (Table 2 in the Supporting Information). There is also a hydrogen bond between the arginine backbone nitrogen atom and a nearby glycerol that stacks with Trp97 (Figure 2). The relatively planar structure of cyclo-(L-Arg-L-Pro) means that hydrophobic stacking with Trp403, also observed in the CI-4 complex, is still possible (Figure 2). In the CI-4 structure the proline carbonyl group is within hydrogen-bonding distance of the hydroxyl group of Tyr214 (Figure 2), although mutation of Tyr214 to phenylalanine showed no reduction in binding of CI-4.[24] A similar hydrogen bond is made with the arginine carbonyl in cyclo-(L-Arg-L-Pro). However, the altered binding orientation means that the backbone nitrogen of the arginine is no longer able to hydrogen bond to a water molecule that is present in the CI-4 structure at a position equivalent to the O6 oxygen of allosamidin's allosamizoline moiety (Figure 2). Instead, the nitrogen is placed in a similar position to the C1 carbon of the allosamizoline moiety. Like CI-4, the arginine side chain does not appear to make any significant contacts with

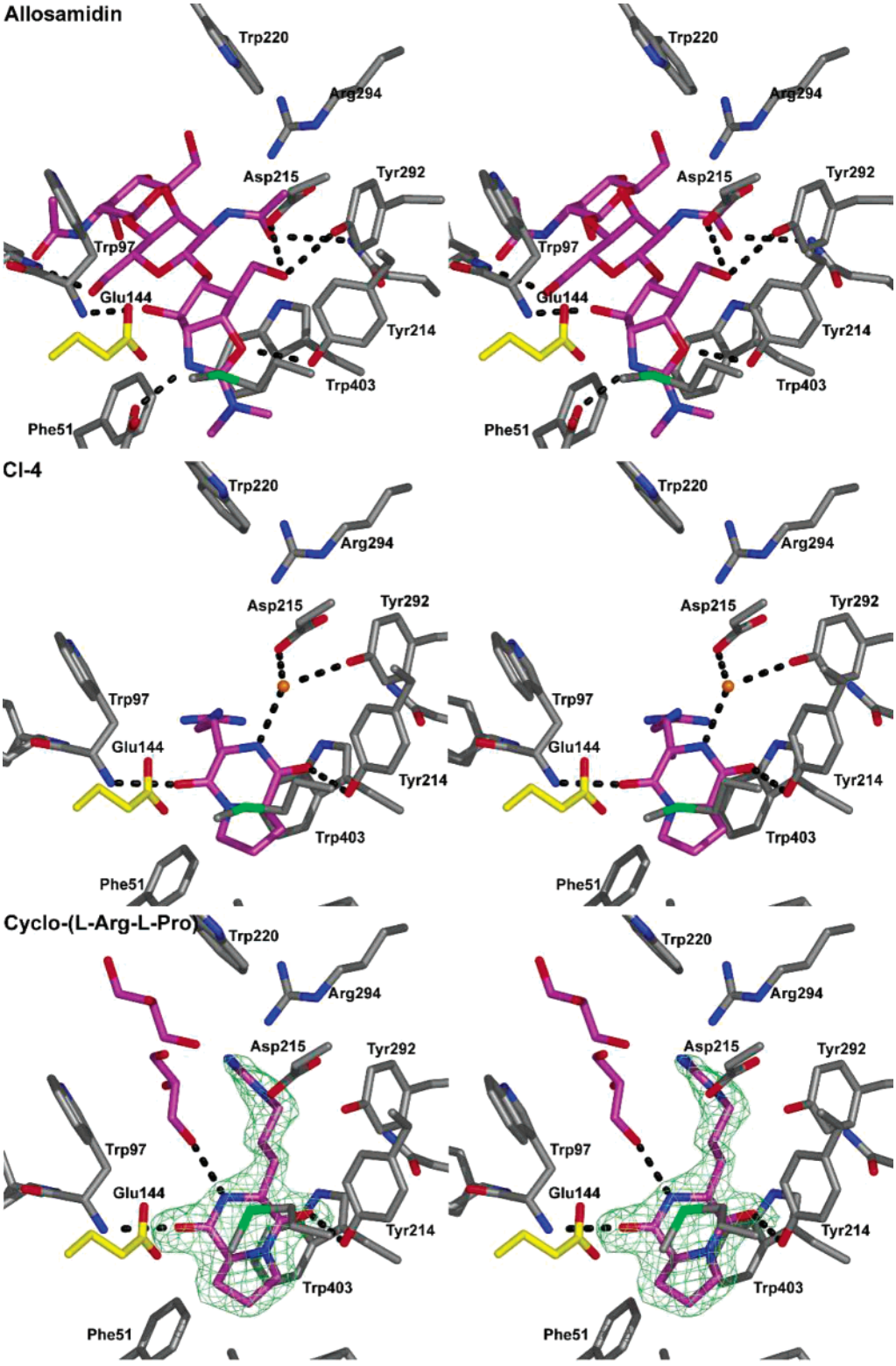


**Figure 2.** Comparison of the complexes with allosamidin,[23] CI-4,[24] and cyclo-(L-Arg-L-Pro). Unbiased $|F_o| - |F_c|$, $\phi_{calc}$ (green mesh, contoured at 2.5$\sigma$) maps are shown for the inhibitors. Amino acids bordering the active site are shown as stick models, and potential hydrogen bonds between the ligands (in the −1 subsite) and protein (including water- or glycerol-mediated) are represented as black dashed lines. The carbon atoms of the catalytic residue (Glu144) are yellow, and those of the ligands are purple. Key water molecules are shown as orange spheres. The figure was made using PYMOL software (DeLano, W. L. The PyMOL Molecular Graphics System (2002) http://www.pymol.org).

the protein (Figure 2). Thus, judged from the structures, the compounds have approximately similar interactions, despite the flip in orientation of the backbone. However, the approximately 5-fold higher $IC_{50}$ for cyclo-(L-Arg-L-Pro) (6.3 mM) compared to CI-4 (Figure 4) suggests that the different orientation of the compounds could play some role. The most likely cause is the water-mediated hydrogen bonds through the ordered water molecule bound near the CI-4 proline nitrogen, which are absent in cyclo-(L-Arg-L-Pro) (Figure 4).

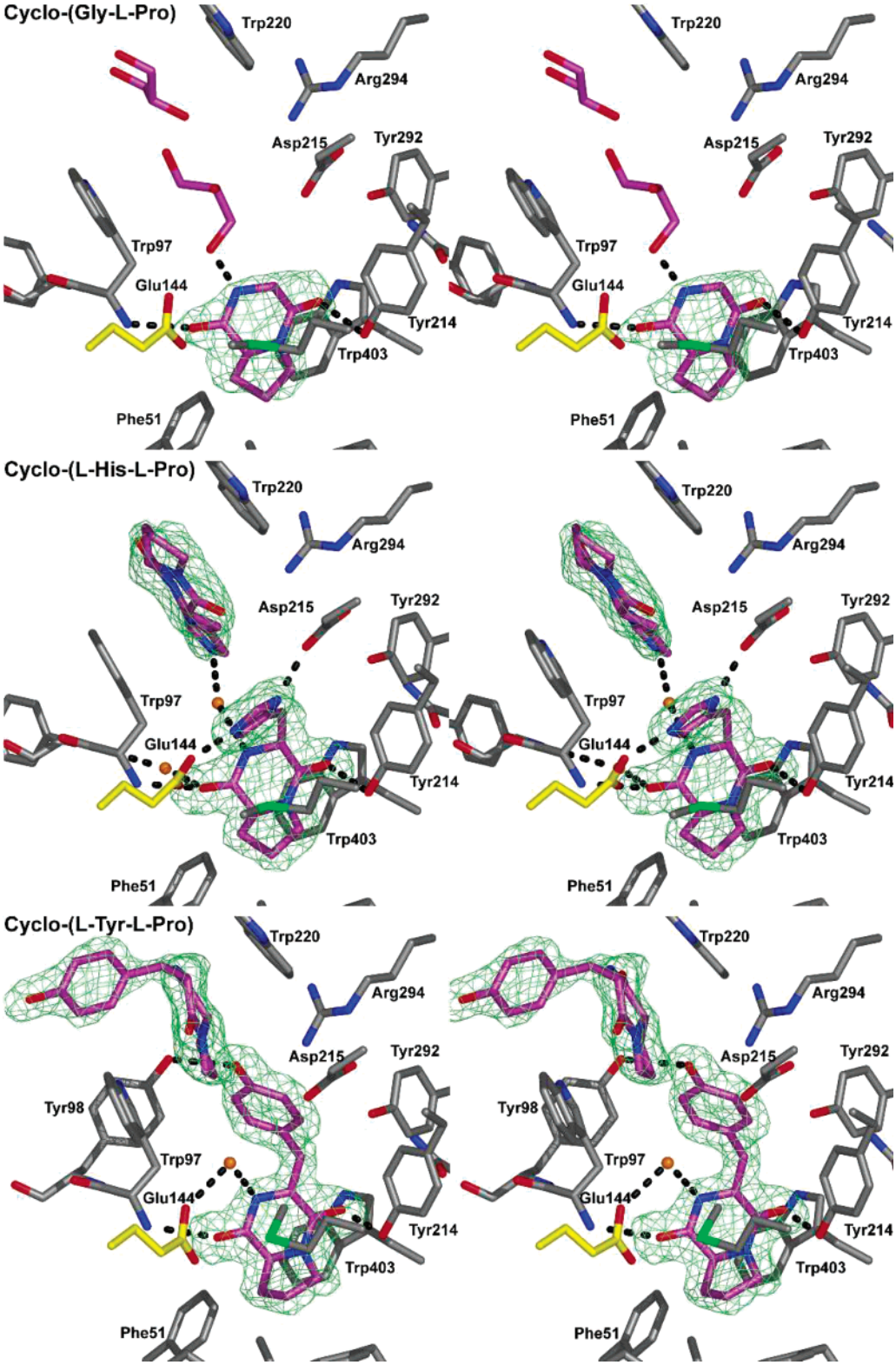


**Figure 3.** Comparison of the complexes with cyclo-(Gly-l-Pro), cyclo-(l-His-L-Pro), and cyclo-(l-Tyr-l-Pro). Unbiased $|F_o| - |F_c|$, $\phi_{calc}$ (green mesh, contoured at 2.5$\sigma$) maps are shown for all inhibitors. Amino acids bordering the active site are shown as stick models, and potential hydrogen bonds between the ligands (in the −1 subsite) and protein (including water- or glycerol-mediated) are represented as black dashed lines. The carbon atoms of the catalytic residue (Glu144) are yellow, and those of the ligands are purple. Key water molecules are shown as orange spheres. The figure was made using PYMOL software (DeLano, W. L. The PyMOL Molecular Graphics System (2002) http://www.pymol.org).

**Cyclo-(Gly-L-Pro).** The observation that the cyclo-(L-Arg-L-Pro) compound still bound and inhibited ChiB prompted us to investigate whether other such dipeptides with the more naturally abundant L-Pro were available. Three compounds were identified, cyclo-(Gly-L-Pro), cyclo-(L-His-L-Pro), and cyclo-(L-Tyr-L-Pro), all available from Sigma. On the basis of the observed backbone flip between CI-4 and cyclo-(L-Arg-L-Pro), we wanted to investigate whether the cyclo-(Gly-L-Pro) substructure alone would inhibit ChiB. ChiB was crys-

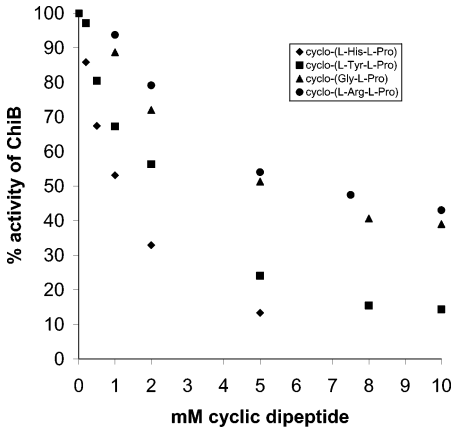


**Figure 4.** Enzymology. The curves show the relative activity of ChiB as a function of peptide concentration. Each point represents the average of three individual measurements. On the basis of these curves, $IC_{50}$ values were estimated as follows: cyclo-(L-His-L-Pro), 1.1 mM; cyclo-(L-Tyr-L-Pro), 2.4 mM; cyclo-(Gly-L-Pro), 5.0 mM; and cyclo-(L-Arg-L-Pro), 6.3 mM. The points for CI-4 were highly similar to those obtained for cyclo-(L-His-L-Pro) and are not shown in the figure. The $IC_{50}$ value for CI-4 was 1.2 mM.

tallized in complex with cyclo-(Gly-L-Pro) and refined to 2.1 Å resolution (Figure 3, Table 1 in the Supporting Information). Cyclo-(Gly-L-Pro) appears to lie in the same orientation as cyclo-(L-Arg-L-Pro) (rmsd = 0.53 Å on equivalent atoms), which was expected as the chirality of the proline α-carbon in cyclo-(Gly-L-Pro) is the same as that in cyclo-(L-Arg-L-Pro) (Figures 1−3). Apart from the two hydrogen bonds with Trp97-N and Tyr214-O$\eta$, there is a hydrogen bond between the backbone nitrogen of the glycine and a nearby glycerol that is stacking with the solvent exposed aromatic residue Trp97 (Figure 3). Overall, the cyclo-(Gly-L-Pro) complex suggests that it is the cyclic dipeptide backbone itself that is the main determinant of binding, as the $IC_{50}$ is 5.0 mM, approximately the same as that for cyclo-(L-Arg-L-Pro) (Figure 4). This also further confirms that the arginine side chain in cyclo-(L-Arg-L-Pro) does not significantly interact with the protein.

**Cyclo-(L-His-L-Pro).** The cyclo-(L-Arg-L-Pro) structure revealed that, although no direct interactions are made, the guanidinium moiety points in the direction of two conserved acidic residues, Asp215 and Glu144 (the catalytic acid) (Figure 2). However, the arginine side chain is too large; it is impossible to find favorable torsion angles that would allow the guanidinium group to form hydrogen bonds with these conserved acidic residues without steric clashes. Histidine, with its shorter, positively charged, side chain, therefore seemed a possible alternative. Cyclo-(L-His-L-Pro) was soaked into a ChiB crystal, and the structure of the complex was refined to 1.90 Å resolution. The cyclic peptide backbone occupies the same space, in the same orientation, as cyclo-(Gly-L-Pro) (Figure 3). In addition to the two standard hydrogen bonds from the dipeptide backbone oxygens, the histidine side chain N$\delta$1 hydrogen bonds Asp215, and N$\epsilon$2 hydrogen bonds with Glu144 (Figure 3, Table 2 in the Supporting Information). The inhibition data show that cyclo-(L-His-L-Pro) is a 5-fold better inhibitor than cyclo-(Gly-L-Pro), with an $IC_{50}$ of 1.1 mM, which is likely to be due to the extra hydrogen bonds formed through the imidazole. However, despite these extra interactions, it is not a better inhibitor than the starting compound, CI-4. A possible explanation is that the $\chi 2$ torsion angle of the histidine side chain is close to an unfavorable eclipsed conformation (Table 3 in the Supporting Information), offsetting the enthalpic gain of the extra hydrogen bonds made by the imidazole. Furthermore, the cyclic backbone is more planar, and thus more strained, than in the other dipeptides (see Supporting Information). Thus, it appears that a more flexible side chain is required if hydrogen bonds are to be formed with Glu144 and Asp215 without forcing the rest of the inhibitor into an unfavorable conformation. For instance, an ornithine side chain may provide a more flexible substitute for the histidine side chain.

There also appears to be a second cyclo-(L-His-L-Pro) molecule binding in the binding cleft, away from the −1 subsite (Figure 3). The unbiased $|F_o| - |F_c|$, $\phi_{calc}$ density for this second molecule was less well defined than that for the first molecule (Figure 3), and after inclusion during refinement, the B-factors refined to an average of 52.9 Å$^2$ for this second molecule, compared to 22.5 Å$^2$ for the first. Although the binding of this additional ligand is likely to be due to the high concentration (70 mM) of the molecule in the soaking solution, its position is interesting in that the cyclic backbone and imidazole ring are stacking with Trp220 and Trp97, respectively (Figure 3). These positions are the +2 and +3 subsites of the enzyme, both of which are occupied by GlcNAc sugars that take up similar stacking arrangements when the substrate is bound.[23] This is in contrast to allosamidin, which occupies the −2 and −3 subsites with the two *N*-acetylallosamine sugars.

**Cyclo-(L-Tyr-L-Pro).** The structure of ChiB shows a number of solvent-exposed aromatic residues lining the active site groove. The complexes of ChiB with $NAG_5$ and allosamidin show that these residues interact with the hydrophobic face of the sugar residues.[23] There is a similar interaction with the phenylalanine side chain of the peptide inhibitor argifin.[25] Cyclo-(L-Tyr-L-Pro) contains an aromatic residue that could make similar interactions. ChiB was crystallized in the presence of cyclo-(L-Tyr-L-Pro) and refined to 1.85 Å resolution. Cyclo-(L-Tyr-L-Pro) binds in the same site and orientation as cyclo-(Gly-L-Pro) and cyclo-(L-Arg-L-Pro) (Figure 3). The structure shows hydrogen bonds similar to all the cyclic dipeptides referred to here (Figure 3). The conformation of the cyclo-(Gly-L-Pro) substructure means that this molecule is the least planar of all the structures discussed (Table 3 in the Supporting Information). The proline ring is puckered in the opposite direction compared to the other cyclic dipeptides, and the backbone is tilted so that, when the structures are superposed, the distance between the proline carbonyl in this structure and the proline carbonyl in the cyclo-(L-His-L-Pro) (the most planar) structure is 1.6 Å. The tyrosine O$\eta$ hydrogen bonds the O$\eta$ of Tyr98 (Figure 3). The side chain of Tyr98 has rotated by approximately 120°, compared to the other complexes, to accommodate this interaction (Figure 3). However, the inhibitor tyrosine side chain makes none of the anticipated stacking interactions with any of the protein side chains (the nearest aromatic side chain that stacks with an GlcNAc sugar in the published substrate complex is Trp97,

**Table 1.** Effect of Inhibitors on Cultured *S. cerevisiae*[a]

| | cell aggregates | | postsonication | | mean cells/ groups |
|---|---|---|---|---|---|
| | mean | SE | mean | SE | |
| no inhibitor | 76.3 | 3.5 | 36.5 | 0.3 | 2.09 ± 0.10 |
| cyclo-(Gly-l-Pro) | 75.7 | 2.5 | 33.2 | 0.4 | 2.28 ± 0.08 |
| cyclo-(l-His-l-Pro) | 90.0 | 2.0 | 32.7 | 0.8 | 2.75 ± 0.09 |
| cyclo-(l-Tyr-l-Pro) | 77.5 | 1.4 | 33.9 | 2.0 | 2.29 ± 0.14 |
| *cts1*Δ | 188.8 | 9.6 | 33.0 | 1.9 | 5.72 ± 0.44 |

[a] Inhibition of chitinase function in vivo was estimated by monitoring the mean particle volume (fl) of yeast cell groups, which increases as cells remain associated due to the failure to digest the primary division septum. Mean particle was calculated over three time points following addition of the cyclic dipeptides (3.25, 5.5, and 7.5 h) and is shown together with the standard error (SE). Clumping of yeast cells indicative of delayed cell separation after division is indicated by the elevated mean particle volume of cell clumps. In comparison, the mean particle volume following disaggregation by mild sonication was very similar in all cultures, showing that the volume of *individual* yeast cells was not changed either by the inhibitors or by the *cts1* deletion. The increased mean volume of yeast cell groups in the presence of cyclo-(L-His-L-Pro) therefore represents a small increase in the average number of cells per group consistent with delayed cell separation.

which is 4.5 Å away from the tyrosine ring). The inhibition studies revealed an $IC_{50}$ of 2.4 mM.

Similar to the structure with cyclo-(L-His-L-Pro) bound, there also appears to be a second cyclo-(L-Tyr-L-Pro) molecule binding nearby, occupying the +1 and +2 subsites and stacking between Trp220 and Trp97 (Figure 3). In this case, there is also a third molecule whose tyrosine ring occupies the −2 subsite. The average *B*-factor for the tyrosine ring in this third molecule is 23.5 Å$^2$, whereas that of the cyclo-(Gly-L-Pro) substructure, which does not interact with the protein, is 36.4 Å$^2$, and the electron density is more disordered around the cyclic backbone than for the relatively well-defined tyrosine ring.

**Activity against *S. Cerevisiae.*** During cell separation the cell walls of the daughter cells of the yeast *S. cerevisiae* are temporarily attached via a chitin-rich septum. The yeast produces and secretes a single (endo)-chitinase, encoded by *CTS1*, which has been shown to be required for proper cell separation, with a *cts1*Δ gene knockout leading to clumps of multiple, unseparated cells.[26] A similar effect is observed when yeast is grown in the presence of an allosamidin derivative.[27] The chitinase is thought to play a role in degrading the septum, thereby allowing the daughter cells to separate.[26] Similarly, chitinases are important for the life cycles of pathogenic fungi, such as *A. fumigatus*.[28] The parent compound, CI-4 (Figure 1), has been shown to affect cell morphology in *C. albicans* and induces a cell-clumping effect, similar to that observed for allosamidin, in cultures of *S. cerevisiae*.[19] We have tested the effect of the cyclic dipeptide inhibitors described here on cell separation of *S. cerevisiae* by directly measuring the average particle volume and relating that to the number of clustered cells, allowing quantitative measurement of the cell-clumping effects described previously. Cultures were grown in the presence and absence of the inhibitors, alongside a *cts1*Δ chitinase knock-out strain as a positive control for complete lack of chitinase activity (Table 1). The increased particle volume for the cyclo-(L-His-L-Pro) culture indicates a statistically significant increase in the number of cells per particle, showing that the cells form small clumps due to inhibition of cell separation by a reduction in the normal chitinolytic activity of the *S. cerevisiae* endochitinase (Table 1). Direct observation of yeast cultures under the microscope (not shown) supported the conclusion that cyclo-(L-His-L-Pro) induced a delay to cell separation.

## Conclusions

The high-resolution structures of ChiB in complex with four novel family 18 chitinase inhibitors presented here have given new insights into the molecular mechanisms of inhibition by cyclic dipeptides and allow interpretation of the inhibition data (Figure 4). The data revealed which features of this class of molecules are the important factors for binding, as well as which features can be modified. As discussed previously,[24] CI-4 and its derivatives interact with residues in the active site that are all conserved throughout the family 18 chitinases, in agreement with the observed activity against both bacterial and fungal chitinases.[18,19,24]

The present structures demonstrate that derivatization of cyclo-(Gly-L-Pro) by the addition of different side chains alters inhibitory properties. It appears that the chirality of the proline determines the orientation of the molecule. We have shown that although the affinity of cyclo-(L-Arg-L-Pro) for ChiB is lower than that of CI-4, comparable interactions are made; the substructure makes two direct hydrogen bonds with the protein, but in neither complex are interactions between the arginine side chain and the protein observed. The cyclo-(Gly-L-Pro) complex demonstrates that the cyclo-(Gly-L-Pro) substructure alone is sufficient for binding. The addition of a histidine residue to this substructure increases affinity due to two extra hydrogen bonds formed with the protein, but this forces the cyclic dipeptide into an unfavorable conformation. The addition of a tyrosine residue also increases affinity versus that of cyclo-(Gly-L-Pro), but the tyrosine side chain is not extended enough to form any stacking interactions with the solvent-exposed aromatic residues in the binding cleft. The results of the in vivo assay against *S. cerevisiae* are compatible with the structural data and the enzyme inhibition assay in that the cyclo-(L-His-L-Pro) appears to be the most potent of all the cyclic dipeptide inhibitors.

In terms of potency, the cyclic dipeptide inhibitors are still 4 orders of magnitude weaker than allosamidin. However, the complexes reveal potential alterations that could be made to the cyclic dipeptide scaffold to make it more allosamidin-like. By retaining the cyclic dipeptide substructure and extending the molecule along the groove-shaped active site, which is so efficiently occupied by allosamidin, an increase in favorable interactions with the protein may be achieved. Thus, such extensions should be composed of groups that mimic the interaction between the *N*-acetylallosamine sugars of allosamidin and the −2/−3 subsites, establishing stacking interactions with the solvent-exposed aromatic residues.[20,23,25] Another significant difference between allosamidin and the cyclic dipeptides is that the latter fail to establish interactions with Asp142, which tightly hydrogen bonds the allosamizoline moiety of allosamidin (Figures 2 and 3). Replacing the cyclic dipeptide proline by a hydroxyproline may allow formation of a hydrogen bond with Asp142. Similarly, methylprolines could more efficiently

occupy the hydrophobic pocket near Ala184, which is fully penetrated by the allosamidin allosamizoline moiety (Figures 2 and 3).

Further derivatization of the cyclic dipeptide scaffold will be explored soon and hopefully lead to the availability of a potent, synthetically accessible chitinase inhibitor.

## Experimental Section

**Synthesis of Cyclo-(L-Arg-L-Pro).** Cyclo-(L-Arg-L-Pro) was synthesized according to methods previously described[18] and was characterized by $^1$H and $^{13}$C NMR and electrospray mass spectrometry. Cyclo-(Gly-L-Pro), cyclo-(L-His-L-Pro), and cyclo-(L-Tyr-L-Pro) were purchased from Sigma (catalog numbers C7280, C3772, and C8607, respectively).

**Purification and Crystallization.** Chitinase B from *S. marcescens* was overexpressed, purified from *Escherichia coli*, and crystallized as described previously,[24,29] in the presence of 70 mM of cyclo-(Gly-L-Pro), cyclo-(L-Arg-L-Pro), or cyclo-(L-Tyr-L-Pro). The crystals were flash-frozen in a nitrogen gas stream. For cyclo-(L-His-L-Pro), a ChiB crystal was placed in a mother liquor solution containing 70 mM of the inhibitor and left to soak for 1 h before freezing. In all cases the mother liquor included 25% glycerol as cryoprotectant.

**X-ray Crystallography.** Diffraction data for the four ChiB−inhibitor complexes were collected at the European Synchrotron Radiation Facility, Grenoble, France (Table 1 in the Supporting Information). After rigid body fitting of the native ChiB model (PDB code 1E15[30]), CNS ("*C*rystallography and *N*MR *S*ystem") software[31] and O[32] were used for iterative rounds of refinement and model building. The models of the ligands were not included until they were fully defined in unbiased $|F_o| - |F_c|$, $\phi_{calc}$ electron-density maps (Figures 2 and 3). PRODRG[33,34] was used to generate coordinates and molecular topologies for the ligands. All four cyclic dipeptides were found in the same location as CI-4,[24] although some displayed additional unexpected binding modes. All were refined at full occupancy. ChiB crystallizes as a dimer;[30] for consistency, comparisons between the complexes are made using the same monomer (chain A). The coordinates and structure factors have been deposited with the PDB (entries 1W1P, 1W1V, 1W1T, and 1W1Y).

**Enzymology.** Enzyme activities of ChiB in the presence of the different cyclic dipeptides were determined using 4-methylumbelliferyl-$\beta$-D-*N*,*N*-diacetylchitobioside as a substrate in a standard assay that has been described previously.[24,29] Reaction mixtures consisted of purified ChiB (2.75 nM), substrate (20 $\mu$M), BSA (0.1 mg/mL), and inhibitor (0−10 mM) in 50 $\mu$L citrate/phosphate buffer pH 6.3. The mixtures were incubated for 10 min at 37 °C (product formation is known to be linear over time under these conditions) and the reaction was stopped by addition of 1.95 mL 0.2 M $Na_2CO_3$. The amount of liberated 4-methylumbelliferone (4-MU) was determined using a DyNA 200 fluorimeter (Hoefer Pharmacia Biotech, San Francisco, CA). Each measurement was performed in triplicate, yielding standard deviations that in all cases were below 5% of the average. $IC_{50}$ values were estimated from plots of relative activity versus inhibitor concentration (Figure 4).

***S. Cerevisiae* Assay.** Two strains of yeast (BY4741, *MAT*a *his3*Δ*1 leu2*Δ*0 met15*Δ*0 ura3*Δ0; Y06947, BY4741 *cts1*::*KanMX6*) were grown overnight in YPD medium at 30 °C, subcultured into fresh medium, and grown to a cell density of ~5 × 10$^6$/mL. Aliquots of the BY4741 culture (840 $\mu$L) were then added to fresh tubes containing 160 $\mu$L of YPD (control) and YPD containing cyclo-(L-Arg-L-Pro), cyclo-(Gly-L-Pro), cyclo-(L-His-L-Pro), or cyclo-(L-Tyr-L-Pro) at 12.5 mg/mL, giving 2 mg/mL final concentration. The culture of the *cts1*Δ strain Y06947 was used as a positive control for the level of cell clumping resulting from complete lack of chitinase activity. Cultures were shaken gently at 30 °C and samples of 135 $\mu$L taken at 0, 3.25, 5.5, and 7.5 h and added to 15 $\mu$L of 37% formaldehyde solution. Particle volume of cell clumps was measured immediately using a Schärfe system CASY cell counter and analyzer and subsequently after brief sonication to dissociate clumps into individual yeast cells. The mean number of yeast cells per clump was estimated from the ratio of particle volume before sonication over particle volume after sonication.

**Acknowledgment.** We thank the European Synchrotron Radiation Facility, Grenoble, France, for the time at beam lines ID14-EH4. DMFvA is supported by a Wellcome Trust Senior Research Fellowship and the EMBO Young Investigator Program. D.R.H. is supported by a BBSRC CASE studentship partially funded by Cyclacel.

**Supporting Information Available:** Tables listing the details of data collection and structure refinement, inhibitor hydrogen bonds, and cyclic dipeptide conformations. This material is available free of charge via the Internet at http://pubs.acs.org.

## References

(1) Huber, M.; Cabib, E.; Miller, L. H. Malaria parasite chitinase and penetration of the mosquito peritrophic membrane. *Proc. Natl. Acad. Sci. U.S.A.* **1991**, *88*, 2807−2810.
(2) Vinetz, J. M.; Dave, S. K.; Specht, C. A.; Brameld, K. A.; Xu, B.; Hayward, R.; Fidock, D. A. The chitinase PfCHT1 from the human malaria parasite *Plasmodium falciparum* lacks proenzyme and chitin-binding domains and displays unique substrate preferences. *Proc. Natl. Acad. Sci. U.S.A.* **1999**, *96*, 14061−14066.
(3) Dickinson, K.; Keer, V.; Hitchcock, C. A.; Adams, D. J. Chitinase activity from candida-albicans and its inhibition by allosamidin. *J. Gen. Microbiol.* **1989**, *135*, 1417−1421.
(4) Cohen, E. Chitin synthesis and degradation as targets for pesticide action. *Arch. Insect Biochem. Physiol.* **1993**, *22*, 245−261.
(5) Arnold, K.; Brydon, L. J.; Chappell, L. H.; Gooday, G. W. Chitinolytic activities in heligmosomoides-polygyrus and their role in egg hatching. *Mol. Biochem. Parasitol.* **1993**, *58*, 317−323.
(6) Villagomezcastro, J. C.; Calvomendez, C.; Lopezromero, E. Chitinase activity in encysting entamoeba-invadens and its inhibition by allosamidin. *Mol. Biochem. Parasitol.* **1992**, *52*, 53−62.
(7) Sakuda, S.; Isogai, A.; Matsumoto, S.; Suzuki, A.; Koseki, K. The structure of allosamidin, a novel insect chitinase inhibitor produced by *Streptomyces sp*. *Tetrahedron Lett.* **1986**, *27*, 2475−2478.
(8) VillagomezCastro, J. C.; LopezRomero, E. Identification and partial characterization of three chitinase forms in Entamoeba invadens with emphasis on their inhibition by allosamidin. *Antonie Van Leeuwenhoek* **1996**, *70*, 41−48.
(9) Sakuda, S.; Isogai, A.; Matsumoto, S.; Suzuki, A. Search for microbial insect growth-regulators. 2. Allosamidin, a novel insect chitinase inhibitor. *J. Antibiot.* **1987**, *40*, 296−300.
(10) Tsai, Y.-L.; Hayward, R. E.; Langer, R. C.; Fidock, D. A.; Vinetz, J. M. Disruption of *Plasmodium falciparum* chitinase markedly impairs parasite invasion of mosuito midgut. *Infect. Immun.* **2001**, *69*, 4048−4054.
(11) Sakuda, S. *Studies on the chitinase inhibitors, allosamidins*, volume 2 of *Chitin Enzymology*; Atec Edizioni: 1996; p 203−212.
(12) Berecibar, A.; Grandjean, C.; Siriwardena, A. Synthesis and biological activity of natural aminocyclopentitol glycosidase inhibitors: mannostatins, trehazolin, allosamidins and their analogues. *Chem. Rev.* **1999**, *99*, 779−844.
(13) Arai, N.; Shiomi, K.; Yamaguchi, Y.; Masuma, R.; Iwai, Y.; Turberg, A.; Koelbl, H.; Omura, S. Argadin, a new chitinase inhibitor, produced by *Clonostachys* sp. FO-7314. *Chem. Pharm. Bull.* **2000**, *48*, 1442−1446.
(14) Shiomi, K.; Arai, N.; Iwai, Y.; Turberg, A.; Koelbl, H.; Omura, S. Structure of argifin, a new chitinase inhibitor produced by *Gliocladium* sp. *Tetrahedron Lett.* **2000**, *41*, 2141−2143.
(15) Blattner, R.; Furneaux, R. H.; Lynch, G. P. Synthesis of allosamidin analogues. *Carbohydrate Res.* **1996**, *296*, 29−40.
(16) Nishimoto, Y.; Sakuda, S.; Takayama, S.; Yamada, Y. Isolation and characterization of new allosamidins. *J. Antibiot.* **1991**, *44*, 716−722.
(17) Kato, T.; Shizuri, Y.; Izumida, H.; Yokoyama, A.; Endo, M. Styloguanidines, new chitinase inhibitors from the marine sponge *Stylotella aurantium*. *Tetrahedron Lett.* **1995**, *36*, 2133−2136.
(18) Izumida, H.; Imamura, N.; Sano, H. A novel chitinase inhibitor from a marine bacterium *Pseudomonas* sp. *J. Antibiot.* **1996**, *49*, 76−80.

(19) Takadera, T.; Nomoto, A.; Izumida, H.; Nishijima, M.; Sano, H. The effect of chitinase inhibitors, cyclo(Arg-Pro) against cell separation of *Saccharomyces cerevisiae* and the morphological change of *Candida albicans*. *J. Antibiot.* **1996**, *49*, 829−831.
(20) Terwisscha, A.; van Scheltinga, C.; Armand, S.; Kalk, K. H.; Isogai, A.; Henrissat, B.; Dijkstra, B. W. Stereochemistry of chitin hydrolysis by a plant Chitinase/lysozyme and X-ray structure of a complex with allosamidin. *Biochemistry* **1995**, *34*, 15619−15623.
(21) Tews, I.; Terwisscha van Scheltinga, A. C.; Perrakis, A.; Wilson, K. S.; Dijkstra, B. W. Substrate-assisted catalysis unifies two families of chitinolytic enzymes. *J. Am. Chem. Soc.* **1997**, *119*, 7954−7959.
(22) Brameld, K. A.; Goddard, W. A. Substrate distortion to a boat conformation at subsite−1 is critical in the mechanism of family 18 chitinases. *J. Am. Chem. Soc.* **1998**, *120*, 3571−3580.
(23) van Aalten, D. M. F.; Komander, D.; Synstad, B.; GÅseidnes, S.; Peter, M. G.; Eijsink, V. G. H. Structural insights into the catalytic mechanism of a family 18 exo-chitinase. *Proc. Natl. Acad. Sci. U.S.A.* **2001**, *98*, 8979−8984.
(24) Houston, D. R.; Eggleston, I.; Synstad, B.; Eijsink, V. G. H.; van Aalten, D. M. F. The cyclic dipeptide CI-4 inhibits family 18 chitinases by structural mimicry of a reaction intermediate. *Biochem. J.* **2002**, *368*, 23−27.
(25) Houston, D. R.; Shiomi, K.; Arai, N.; Omura, S.; Peter, M. G.; Turberg, A.; Synstad, B.; Eijsink, V. G. H.; van Aalten, D. M. F. High-resolution structures of a chitinase complexed with natural product cyclopentapeptide inhibitors: Mimicry of carbohydrate substrate. *Proc. Natl. Acad. Sci., U.S.A.* **2002**, *99*, 9127−9132.
(26) Kuranda, M. J.; Robbins, P. W. Chitinase is required for cell-separation during growth of *Saccharomyces cerevisiae*. *J. Biol. Chem.* **1991**, *266*, 19758−19767.
(27) Sakuda, S.; Nishimoto, Y.; Ohi, M.; Watanabe, M.; Takayama, S.; Isogai, A.; Yamada, Y. Effects of demethylallosamidin, a potent yeast chitinase inhibitor, on the cell-division of yeast. *Agr. Biol. Chem. Tokyo* **1990**, *54*, 1333−1335.
(28) Takaya, N.; Yamazaki, D.; Horiuchi, H.; Ohta, A.; Takagi, M. Cloning and characterization of a chitinase-encoding gene chiA from *Aspergillus nidulans*, disruption of which decreases germination frequency and hyphal growth. *Biosci. Biotechnol. Biochem.* **1998**, *62*, 60−65.
(29) Brurberg, M. B.; Nes, I. F.; Eijsink, V. G. H. Comparative studies of chitinases A and B from *Serratia marcescens*. *Microbiology* **1996**, *142*, 1581−1589.
(30) van Aalten, D. M. F.; Synstad, B.; Brurberg, M. B.; Hough, E.; Riise, B. W.; Eijsink, V. G. H.; Wierenga, R. K. Structure of a two-domain chitotriosidase from *Serratia marcescens* at 1.9 Å resolution. *Proc. Natl. Acad. Sci. U.S.A.* **2000**, *97*, 5842−5847.
(31) Brunger, A. T.; Adams, P. D.; Clore, G. M.; Gros, P.; Grosse-Kunstleve, R. W.; Jiang, J.-S.; Kuszewski, J.; Nilges, M.; Pannu, N. S.; Read, R. J.; Rice, L. M.; Simonson, T.; Warren, G. L. Crystallography and NMR system: A new software system for macromolecular structure determination. *Acta Crystallogr.* **1998**, *D54*, 905−921.
(32) Jones, T. A.; Zou, J. Y.; Cowan, S. W.; Kjeldgaard, M. Improved methods for building protein models in electron density maps and the location of errors in these models. *Acta Crystallogr.* **1991**, *A47*, 110−119.
(33) Kleywegt, G. J.; Henrick, K.; Dodson, E. J.; van Aalten, D. M. F. Pound-wise but penny-foolish: How well do micromolecules fare in macromolecular refinement? *Structure* **2003**, *11*, 1051−1059.
(34) Schuettelkopf, A. W.; van Aalten, D. M. F. PRODRG: A tool for high-throughput crystallography. *Acta Crystallogr.* **2004**, *D60*, 1355−1363.

JM049940A